UC Santa Barbara

UC Santa Barbara Previously Published Works

Title

Balancing the last glacial maximum (LGM) sea-level budget

Permalink

https://escholarship.org/uc/item/94t57148

Authors

Simms, Alexander R
Lisiecki, Lorraine
Gebbie, Geoffrey
et al.

Publication Date

2019-02-01

DOI

10.1016/j.quascirev.2018.12.018

Peer reviewed

Balancing the last glacial maximum (LGM) sea-level budget

Alexander R. Simms [a, *], Lorraine Lisiecki [a], Geoffrey Gebbie [b], Pippa L. Whitehouse [c], Jordan F. Clark [a]

[a] *Department of Earth Science, University of California Santa Barbara, 1006 Webb Hall Santa Barbara, CA, 93106, USA*
[b] *Department of Physical Oceanography, Woods Hole Oceanographic Institution, Woods Hole, MA, 02543, USA*
[c] *Department of Physical Geography, Durham University, South Road, Durham, DH1 3LE, UK*

ARTICLE INFO

ABSTRACT

Estimates of post-Last Glacial Maximum (LGM) sea-level rise are not balanced by the estimated amount of ice melted since the LGM. We quantify this "missing ice" by reviewing the possible contributions from each of the major ice sheets. This "missing ice" amounts to 18.1 ± 9.6 m of global sea-level rise. Ocean expansion accounts for 2.4 ± 0.3 m of this discrepancy while groundwater could contribute a maximum of another 1.4 m to this offset. After accounting for these two potential contributors to the sea-level budget, the shortfall of 15.6 ± 9.6 m suggests that either a large reservoir of water (e.g. a missing LGM ice sheet) has yet to be discovered or current estimates of one or more of the known LGM ice sheets are too small. Included within this latter possibility are potential inadequacies of current models of glacial isostatic adjustment.

1. Introduction

Constraining the amount of sea-level rise since the Last Glacial Maximum (LGM) is important for monitoring current ice sheets (Shepherd et al., 2012), understanding early human migrations (Lambeck et al., 2011), and calibrating models (Peltier, 1994; Kageyama et al., 2006) and geochemical proxies (Mix, 1987). Two approaches are generally used to reconstruct sea levels during the LGM. Early attempts used a direct approach, which dated ancient shoreline features or sea-level "index" points (Fairbanks, 1989; Yokoyama et al., 2000) in areas thought to be far enough away from the past ice sheets as to represent the global "average" sea level, which in turn is representative of the total ocean volume change (i.e., ice-equivalent sea-level change)(Fairbanks, 1989). This approach has since been improved by accounting for glacial isostatic adjustment (GIA), which is the deformation of the Earth's surface and gravitational field (hence equipotential) due to the redistribution of ocean, ice, and mantle material during the growth and decay of ice sheets. GIA can be important even at sites far away from the LGM ice sheets (Peltier, 1994; Lambeck and Chappell, 2001; Austermann et al., 2013). The second approach is to reconstruct the configuration of the LGM ice sheets and sum the volume of water stored above flotation at the LGM (Denton and Hughes, 1981; Clark and Tarasov, 2014). However, these two approaches are not necessarily independent of one another as the second approach is used to determine the GIA component of sea-level change and hence improve sea-level estimates derived from the first approach (Lambeck and Chappell, 2001).

Direct measurements of the elevation of sea level at the LGM are based largely on estimates from Barbados (Fairbanks, 1989; Austermann et al., 2013), the Sunda Shelf (Hanebuth et al., 2000), and the Bonaparte Gulf (Yokoyama et al., 2000). When corrected for GIA (Lambeck et al., 2014; Nakada et al., 2016), including the impacts of 3-dimensional heterogeneity within the mantle (Austermann et al., 2013), these records [typically] imply a LGM lowstand between 130 m and 134 m. In contrast, although the amount of ice within each individual ice sheet at the LGM is still a matter of debate, the various estimates of the ice-equivalent sea-level change locked up in the LGM ice sheets sum to considerably less than 130 m (Clark and Tarasov, 2014) (Table 1; Figs. 1 and 2). The first global compilation (Denton and Hughes, 1981) of ice sheets at the LGM suggested they account for between 127 and 163 m of ice-equivalent sea-level change, but as field mapping and dating methods have improved over the years, particularly within Antarctica, those estimates have generally decreased (Table 1).

This problem has led several authors to argue for a hypothetical

Table 1
Estimates of the meltwater contributions from individual ice sheets listed in order of publication.

SL contribution (m)	Error (m)	Reference	Average (m)	s (m)
		North America		
74	4	Peltier (2004)	*(post-2000)*	
79	2	Lambeck and Purcell (2005)	75.4	5.7
80 (70)	8'	Tarasov et al. (2012)		
79"	5*	Gregoire et al. (2012)		
66**	5*	Simon et al. (2016)	*(post-2010)*	
79	5@	Lambeck et al. (2017)	76.0	6.7
		Eurasia		
17	0.85*	Peltier (2004)	*(post-2000)*	
21	0.85*	Lambeck et al. (2006)	18.7	3.8
17.2	0.7	Peltier et al. (2015)		
14.4	1	Root et al. (2015)		
24	1	Hughes et al. (2016)	*(post-2010)*	
18.1#	0.85	Patton et al., 2016	18.4	4.9
		Antarctica		
20	1.45*	Nakada et al. (2000)		
17.5	3.5	Huybrechts (2002)		
17.3	1.45*	Peltier (2004)		
10.12	1.45*	Ivins et al. (2005)		
16.8	1.45*	Peltier and Fairbanks (2006)	*(post-2000)*	
27.85	1	Bassett et al. (2007)	13.2	5.6
10.2	1.45*	Mackintosh et al., 2011$		
9	1.45*	Whitehouse et al. (2012)		
9.2	0.5	Gomez et al. 2013&		
8.3	1.3	Golledge et al. (2013)		
7.5	1.45*	Ivins et al. (2013)		
10.5	1.45*	Golledge et al. (2014)		
10	4.35	Briggs et al. (2014)		
10.7	1.5	Maris et al. (2014)	*(post-2010)*	
13.6	1.45*	Argus et al. (2014)	9.9	1.7
		Greenland		
2.7	0.8	Huybrechts (2002)		
3.1	0.5*	Fleming and Lambeck (2004)		
2.6	0.5*	Peltier (2004); Tarasov and Peltier (2002)	(post-2000)	
4.1	0.5*	Simpson et al. (2009)	3.5	0.9
3	0.5*	Peltier et al. (2015)		
4.7	0.5*	Lecavalier et al. (2014)	*(post-2010)*	
4.6	0.7	Khan et al., 2016	4.1	1.0
		Small ice caps		
5.5	0.5	Denton and Hughes (1981); Peltier et al. (2015)	5.5	0.5
		Post 2000 Total	116.4	8.9%
		Post 2010 Total	113.9	8.6%

'Enlarged to encampus another possible solution of 73.9 ± 4 discussed in the study.
"Assumes 7% greater ice volume than Ice-5G.
*No error provided. Assumed an error equivalent to the average of the errors provided by other estimates of the same ice sheet.
**assummed 8 m less than Ice-5G.
@Based on the spread of other solutions suggested in the paper.
#based on a conversion of 2.519 m/106 km^3 ice Briggs et al. (2014)..
$Largest extent model - value from Ivins et al. (2013).
&based on the reduced sliding coefficient ice-sheet model.
%Based on the square root of the sum of the squares (see text).

"missing ice sheet" potentially over the present-day East Siberian margin (Clark and Tarasov, 2014). However, before searching for a yet undiscovered ice mass, it is important to review the other contributors to global sea-level rise; namely, the contributions to sea-level change caused by global ocean density changes accompanying ocean warming and freshening since the LGM and potential groundwater storage. The purpose of this paper is to 1.) quantify the amount of missing ice, 2.) discuss the possible role of ocean warming in the sea-level budget at the LGM in context with an accompanying paper (Gebbie et al., in review), 3.) provide an estimate for the maximum contribution of groundwater to the LGM sea-level budget, and 4.) discuss future directions for addressing the "missing ice" problem.

2. Quantifying LGM ice volumes

2.1. Current estimates of LGM ice volumes

Most early studies that sought to balance the LGM sea-level budget assumed that the volume of ice leftover after accounting for the ice held within the North American, Greenland, and Eurasian Ice Sheets should be attributed to the Antarctic Ice Sheet (Nakada and Lambeck, 1988; Peltier, 1994; Nakada et al., 2000). However, based on the relatively modest (<32 m) elevation of raised beaches across Antarctica, Colhoun et al. (1992) suggested only minimal expansion of the Antarctic Ice Sheet across the continental shelf at the LGM, sufficient to explain only 0.5–2.5 m of the
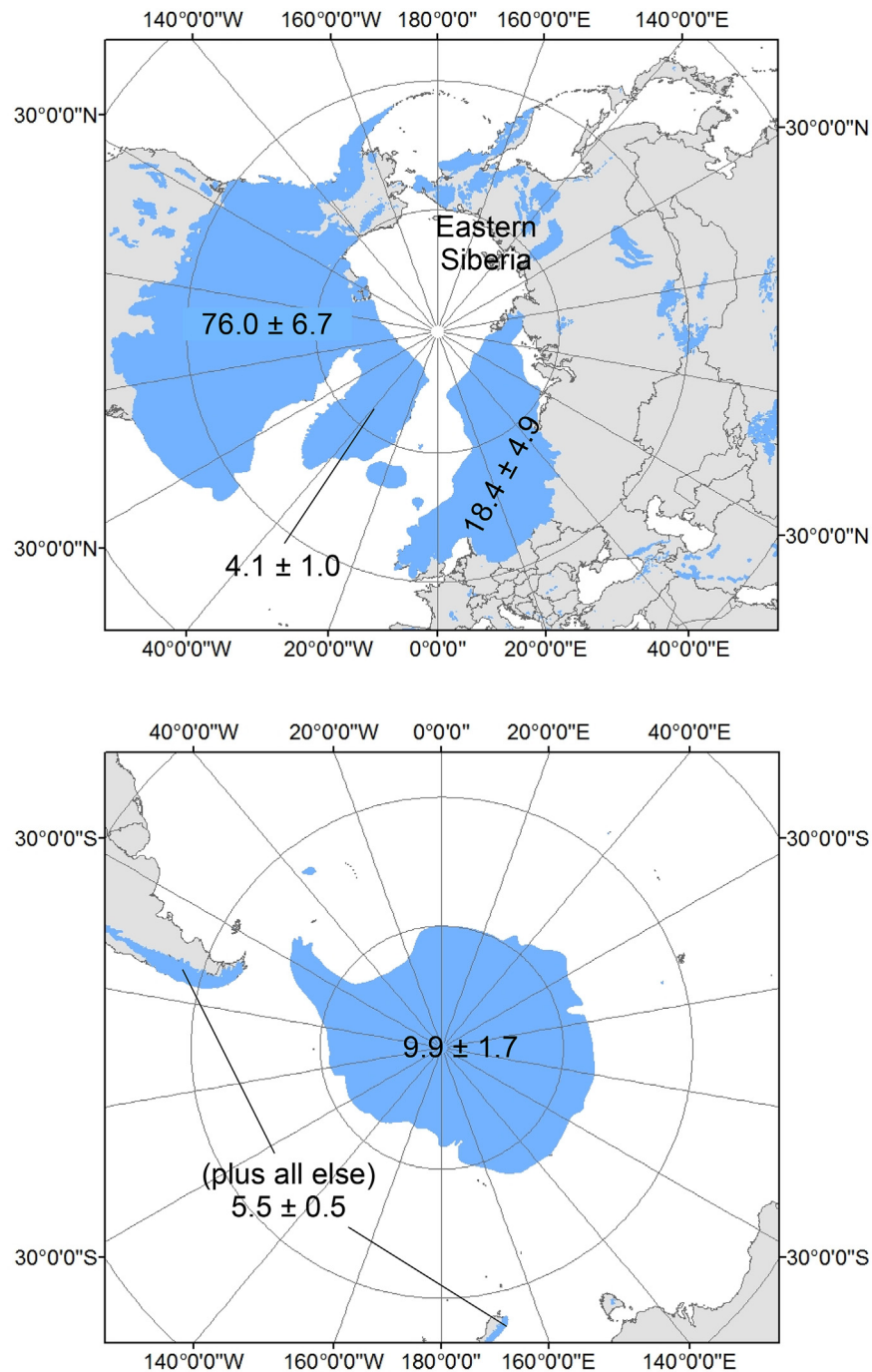
Fig. 1. Maps of the polar regions showing the distribution of ice during the LGM and their approximate contributions to ice-equivalent sea-level rise since the LGM based on post-2010 studies (Table 1). The ice extents are based on those summarized by Ehlers et al. (2011).

LGM lowstand. This led Andrews (1992) to pose the question "where is the missing water?"

Offshore studies have subsequently documented significant ice sheet expansion out to the continental shelf edge over many parts of Antarctica (Anderson et al., 2002, 2013; The RAISED Consortium et al., 2014), but the LGM volume of this ice sheet is still poorly constrained. Based on GIA model predictions of near-field relative sea-level change, Bassett et al. (2007) inferred a post-LGM sea-level contribution of 27.15 m from Antarctica; sufficient to close the global sea-level budget (Table 1). However, GIA modeling studies

that additionally seek to honor glacial geological constraints on past Antarctic ice thickness yield smaller estimates of 7.5–13.6 m (Ivins and James, 2005; Whitehouse et al., 2012b; Ivins et al., 2013; Argus et al., 2014)(Table 1). Several recent studies use numerical modeling techniques to estimate the volume of the LGM ice sheet (Whitehouse et al., 2012a; Golledge et al., 2013; Gomez et al., 2013; Maris et al., 2014; Briggs et al., 2014), and these typically also yield relatively low values (Table 1).

Based on studies published since 2010, the average post-LGM sea-level contribution from Antarctica is estimated to be 9.9 ±
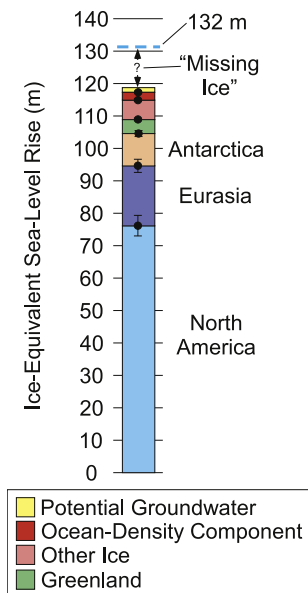
Fig. 2. Bar graph illustrating the disparity between the estimated amount of ice held within the ice sheets and the total ice-equivalent sea-level rise since the LGM. See Table 1 for a list of estimates for the ice-equivalent sea-level rise stored in each of the major ice sheets.

1.7 m (one standard deviation; Table 1). Estimates of the total ice-equivalent sea-level rise held within the other large ice sheets at the LGM have remained relatively steady over the past ~20 years, with 76.0 ± 6.7 m and 18.4 ± 4.9 m post-LGM sea-level rise predicted to have been sourced from North America and Fennoscandia, respectively (Table 1). The exception is the estimate by Simon et al. (2016), which suggests a much smaller LGM North American Ice Sheet complex (Table 1). Excluding Simon et al. (2016), the average sea-level contribution from the North American Ice Sheet complex is 79.3 m instead of 76.0 m. Estimates of Greenland's contribution have increased but it remains a minor component of the sea-level budget at the LGM (Table 1). All other ice masses are thought to have contributed no more than 5.5 ± 0.5 m sea-level rise since the LGM (Denton and Hughes, 1981; Peltier et al., 2015).

2.2. Ice volume to sea-level rise conversions

The compiled studies of meltwater volume differ in the methods used to convert from ice volume to ice-equivalent sea-level rise. With the exceptions of the studies by Ivins and James (2005) and Lambeck et al. (2014), the conversions used ranged between 2.466 and 2.519 m/10^6 km^3 of ice, which would cause variations in ice-equivalent sea-level rise of less than 2.8 m assuming a post-LGM change in ice volume of 52 × 10^6 km^3 (Table 2).

However, the conversion by Lambeck et al. (2014) results in 5.8 m more sea-level rise than that of Hughes et al. (2016) at the LGM. This discrepancy in converting ice to sea level partly arises from the assumed shape and area of the ocean since the LGM. Some studies (e.g. Denton and Hughes, 1981; Hughes et al., 2016) use an ocean area equivalent to the modern ocean area while others account for the changing shape of the ocean as it floods the continental shelf through the deglaciation (e.g. Lambeck et al., 2014). This difference in approaches is nontrivial as the difference between using a modern ocean area (3.619 × 10^8 km^2; Eakins and Sharman, 2010) versus an LGM ocean area (~3.385 × 10^8 km^2 using ICE-5G with the VM2 earth model) is 9 m of ice-equivalent sea-level rise for the same volume of ice (assuming an ice-ocean density ratio of 0.89 and an ice volume of 52 × 10^6 km^3). Determining an appropriate ocean shape and area to use is not a trivial problem (Peltier, 1994; Milne et al., 2002; Mitrovica, 2003; Gomez et al., 2013). One of the complications in determining the shape and area of the ocean is the influence of Earth deformation due to changes in ice and water loading (Milne et al., 1999). Further complications arise when considering the influence of marine-based ice on LGM ocean areas (Milne et al., 1999).

Another source of discrepancy among conversions may arise from different assumptions about which portions of ice sheets contributed to the rise in sea levels. Not all additional ice (e.g. marine-grounded ice below flotation) contributes to sea-level rise (Milne et al., 1999). Thus, some ice should not be included in the equivalent sea-level rise term and may bias the average conversion calculated using the volume of additional ice at the LGM, thus making a uniform conversion from additional ice to an equivalent sea-level rise inappropriate. As not all studies stated what conversions were used and some conversions are based on quoted volumes of additional LGM ice that include both floating and grounded ice, we have not accounted for this discrepancy in our analysis but note an additional offset of up to ~5 m (but likely closer to 2 m) may be due to differences in the ice to seawater conversion.

2.3. Shortfall in the LGM ice sheet volumes

We estimate the amount of "missing ice" at the LGM by averaging the contributions of each ice sheet to the total meltwater budget from only those studies published since 2010. Implicit in this approach is the assumption that all the ice sheets reached their largest LGM configurations at the same time, which is incorrect. For example the Eurasian Ice Sheet likely reached its maximum ice extent at 21 ka (Hughes et al., 2016) while the North American Ice Sheets reached their maximum extent 22 ka (Stokes et al., 2016) or potentially even earlier (e.g. Tarasov et al., 2012). However, by assuming they all reached their largest LGM configuration at the same time, we are able to place constraints on the maximum contribution from the ice sheets. By limiting our analysis to only those studies published since 2010, we also assume that with time,

Table 2
Selected conversions from ice volume to ice-equivalent sea-level rise from previous studies.

Source	Conversions (m SL/km^3 ice)	LGM ice-equivalent sea-level rise**
Denton and Hughes (1981)	2.485	129.2
Ivins et al. (2005)	2.580	134.2
Tarasov et al. (2012)*	2.519	131.0
Golledge et al. (2013)	2.478	128.8
Lambeck et al. (2014)	2.577	134.0
Maris et al. (2014)	2.488	129.4
Hughes et al. (2016)	2.466	128.2

*state 25.19 but assumed 2.519 (Briggs et al., 2014).
**Assuming 52 × 10^6 km^3 of ice (Lambeck et al., 2014).

and presumably more data and better models, estimates are improving. We also assumed that all the models were independent and all of similar validity. This assumption is clearly incorrect and future efforts should attempt to weight better-constrained ice-sheet models more strongly than weaker models. In the absence of published probability distribution functions for most of the studies, we also assumed a Gaussian distribution to the sea-level contributions. As a starting point, we make these assumptions, which results in a value of 113.9 ± 8.5 m of ice-equivalent sea level held within the ice sheets (Table 1). Although not ideal, the error quoted assumes that the uncertainty of each ice sheet's size is equal to the standard deviation of estimates published since 2010. As an alternative approach, we applied a Monte Carlo simulation by randomly selecting LGM ice volumes from the published estimates and the potential ice volumes within the ranges set by their uncertainties. This approach yields the same mean of 113.9 m with a standard deviation of 9.4 m and a 95% confidence interval of 95.1—131.7 m (Fig. 3). Only 3.8% of the sampled totals lead to an ice-equivalent sea-level rise of 130 m or greater. Our calculations include the contributions from the major ice centers in North America, Eurasia, Antarctica, and Greenland, as well as a 5.5 ± 0.5 m contribution from smaller ice caps across other areas in the Northern and Southern Hemispheres (Denton and Hughes, 1981; Peltier et al., 2015). Assuming a post-LGM global mean sea-level change of 132±2 m leaves a discrepancy of 18.1 ±9.6 m (one standard deviation using the Monte Carlo simulation) and a nominal 95% confidence interval of −0.1−37.3 m of unaccounted-for ice needed to balance the sea-level budget during the LGM (Fig. 3).

3. Ocean density changes at the LGM

3.1. Density changes in the LGM ocean

One potential contribution to deglacial sea-level rise not considered in previous studies is ocean expansion due to density changes in the global oceans. The factors responsible for LGM ocean density changes include temperature, salinity, and loading (or compressibility) of the underlying oceans by the added meltwater since the LGM. The most direct effect is that of temperature. This effect originates from the increasing density with decreasing temperature of saltwater, which unlike freshwater does not experience a maximum density at 4 °C. Several approaches have been taken to estimate past ocean temperatures. These make use of a range of records, including the $\delta^{18}O$ record of marine sediments, microfossil-based transfer functions, planktonic Mg/Ca paleothermometers, alkenones, noble gas ratio records from ice cores, and pore-fluid measurements of Cl and $\delta^{18}O$ of seawater.

The three most widely accepted approaches to determining the temperature of the global oceans during the LGM include the work of Clark et al. (2009), MARGO Project Members (2009), and Adkins et al. (2002). Clark et al. (2009) subtracted an assumed sea-level $\delta^{18}O$ signal - based on 127.5 ± 7.5 m of assumed sea-level change - from the global seawater $\delta^{18}O$ signal derived from Lisiecki and Raymo (2005). The residual $\delta^{18}O$ signal suggests that the LGM deep-ocean average global temperature was 3.25 ± 0.55 °C cooler than present. The second approach by the MARGO Project Members (2009) compiled site-specific proxy measurements of LGM
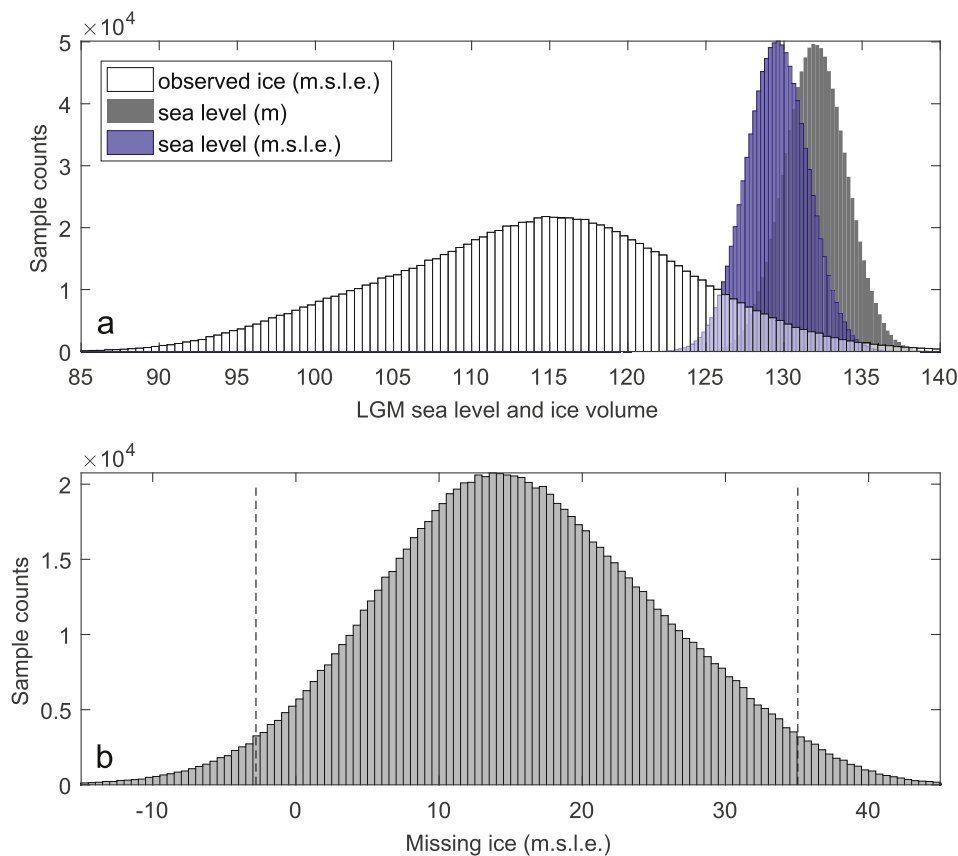
Fig. 3. (Top) White histogram shows estimates for total observed ice based on randomly sampling an estimate of each ice sheet's size from among the published values (Table 1). The dark gray histogram is expected ice based on GIA-corrected sea-level estimates (132± 2). The Blue histogram is the sea-level estimate after correcting for the ocean-density effect (Fig. 4). (Bottom) Histogram illustrating the "missing ice" defined as the expected ice (blue histogram − top panel) minus the observed ice (white histogram-top panel) minus the groundwater/lake change (not shown). The missing ice estimate has a mean of 15.6 m and a 95% confidence range of −2.6−34.9 m. 4.7% of the samples are zero or less (i.e., requiring no missing ice).

temperature change across the globe. They estimated that the global average surface ocean temperature was $1.9 \pm 1.8\,°C$ cooler during the LGM. The third study by Adkins et al. (2002) used Cl and $\delta^{18}O$ measurements within seafloor porewater coupled with foraminiferal $\delta^{18}O$ to calculate intermediate and deep water temperatures at four sites. The latter two studies found that temperature change between the LGM and present varied with respect to depth within the oceans as well as location within the major ocean basins (Adkins et al., 2002; MARGO Project Members, 2009). MARGO Project Members (2009) found that Atlantic surface temperatures changed by $2.4 \pm 2.2\,°C$ since the LGM and Pacific sea surface temperatures changed by $1.5 \pm 1.8\,°C$ since the LGM. The deeper oceans may have seen even larger changes: pore fluid-based estimates suggest the deep Atlantic was $4.0 \pm 0.5\,°C$ cooler during the LGM and the deep Southern Ocean was $1.7 \pm 0.9\,°C$ cooler (Adkins et al., 2002). A more recent estimate by Bereiter et al. (2018) uses noble gases trapped within ice cores to estimate an average ocean temperature of $2.57 \pm 0.24\,°C$ cooler during the LGM.

Another potential influence on past ocean densities is salinity change due to dilution. Estimates of the decrease in ocean salinity since the LGM vary from $0.95 \pm 0.03\,g/kg$ in the Deep Atlantic to $2.40 \pm 0.17\,g/kg$ in the Southern Ocean (Adkins et al., 2002). The single intermediate-depth estimate from the Atlantic Ocean suggests a $1.16 \pm 0.10\,g/kg$ change (Adkins et al., 2002). However, the effect of salinity change on seawater density must be calculated carefully. Munk (2003) points out that studies of ongoing sea-level rise due to recent ocean warming must take care not to count the salinity effect twice − once by adding the volume of meltwater assuming a density of freshwater and a second time by correcting for a salinity change to the rest of the ocean. The third important factor controlling ocean density changes is the compression of the deep ocean by the additional ~130 m of sea level. This effect compensates for some of the post-LGM expansion that arises due to ocean warming (Gebbie et al., in review).

3.2. Impacts of ocean density changes on global sea-level rise

In a companion study, Gebbie et al. (in review) use a 3-dimensional ocean inverse model to investigate the relative roles of temperature change, salinity change, and meltwater loading on LGM ocean density and post-LGM sea-level rise. They consider four different scenarios of LGM ocean conditions and determine the reduction in the amount of ice required to obtain a sea-level rise of 130 m after accounting for ocean expansion. Specifically, we define the ocean density effect of sea-level change in each scenario as $\eta - \eta_{ice}$, where η is the total sea-level rise of 130 m and η_{ice} is the sea-level rise due to the extra volume of water held in the ice sheets. All four scenarios of the LGM temperature and salinity fields are constrained by sea-surface temperature estimates from the MARGO Project Members (2009). In addition, one of them (G12) is also constrained by the porewater measurements of Adkins et al. (2002) and $\delta^{18}O$ constraints (Gebbie, 2012). Two of these scenarios (G14, G14A) are constrained by over 241 $\delta^{18}O$ measurements as well as $\delta^{13}C$ and Cd/Ca measurements (Gebbie, 2014). The fourth scenario contains additional $\delta^{18}O$ and $\delta^{13}C$ measurements but not Cd/Ca measurements (Gebbie et al., 2015). In the 4 scenarios, the global mean temperature profiles have different vertical structures, but they show an ocean warming of $1.0-3.5°$ over the deglaciation consistent with the proxy measurements (Adkins et al., 2002). Gebbie et al. (in review) arrive at values of 2.56, 2.36, 2.06, and 1.96 m for the ocean density effect (Gebbie et al., in review).

Gebbie et al. (in review) also show that these values of the ocean-density effect are well explained by a linear function of temperature and salinity change in the water that remained in the ocean throughout the glacial cycle (i.e. not including the ~130 m-thick layer converted from ice since the LGM). Here we reformulate their analysis and relate it to the difference in global-mean temperature at all depths including that added due to ice-sheet melting, thus a $0.4\,°C$ offset with the regression analysis in their study. In this way, the results can be used in combination with any current or future estimates of global ocean temperature change since the LGM (e.g. Bereiter et al., 2018). We assume that the temperature change is well represented by $\overline{\theta}_m - \overline{\theta}_g$, the LGM ($\overline{\theta}_g$) -to-modern ($\overline{\theta}_m$) change in global-mean Conservative Temperature (units of $°C$). We assume that the deglacial freshening and pressure increased by the same amount in all four scenarios. Any addition of salt is detectable if the LGM global-mean salinity is different from that expected by dilution:

$$S' = \overline{S}_m - \overline{S}_g + 1.16\,g/kg, \tag{1}$$

where S' is a salinity measure of the imbalance, $\overline{S}_m$ is the salinity of the modern ocean, $\overline{S}_g$ is the salinity of the LGM ocean, and $1.16\,g/kg$ is the expected salinity change without any deglacial source.

Putting this together, we hypothesize that the ocean-density effect ($\eta - \eta_{ice}$), assuming salt is conserved (see Gebbie et al., in review, for the case where salt is not conserved), is explained by the following linear equation,

$$\eta - \eta_{ice} \approx a_1 (\overline{\theta}_m - \overline{\theta}_g) + a_2, \tag{2}$$

where a_1 and a_2 represent the effects of the addition of heat and mass, respectively. Given the four scenarios of Gebbie et al. (in review), we have four independent constraints on the two unknown coefficients. Using an overdetermined least squares method, we find that $a_1 = 0.52 \pm 0.01\,m/°C$ and $a_2 = 1.00 \pm 0.04\,m$. This linear function of global-mean quantities reproduces the 3D ocean model analysis of Gebbie et al. (in review) with a root-mean-square error of less than 4 cm.

The coefficient, a_1, gives the sensitivity of sea-level rise to the LGM-to-modern temperature change. The positive value of a_1 indicates that the more the deglacial ocean warms, the more it expands, and the less meltwater (greater values of $\eta - \eta_{ice}$) is needed to give the assumed 130 m of sea-level rise. The coefficient, a_2, is positive due to expansion caused by the seawater becoming less saline due to dilution by meltwater, but this effect is partially compensated by contraction due to the increase in pressure (Gebbie et al. in review).

We use these regression results to assess the uncertainty in the expansion of the ocean due to warming since the LGM. Assuming salt is conserved (e.g., $\overline{S}_m - \overline{S}_g = -1.16\,g/kg$), and that global-mean ocean temperature change ($\overline{\theta}_m - \overline{\theta}_g$) was $2.57 \pm 0.24\,°C$, the regression predicts an ocean-density effect of $2.2-2.5\,m$ (Fig. 4). This estimate can be broken down into the individual temperature and mass contributions using the coefficients within Equation (2). The temperature contribution is simply a_1 multiplied by the warming, or 1.3 m. The second term, a_2 or 1.0 m, arises from three quantities caused by adding mass to the ocean. These include the deglacial increase in freshwater, the additional loading of the ocean due to sea-level rise, and an offset to account for the differences in densities between freshwater and seawater. Gebbie et al. (in review) discusses in detail how these three quantities factor together. As the Bereiter et al. (2018) study is not the only estimate of global LGM ocean cooling, we also consider those of Clark et al. (2009) ($3.25 \pm 0.55\,°C$) and Elderfield et al. (2012) ($2.5 \pm 1.0\,°C$). Using these estimates gives a more conservative error range of $1.8-3.0\,m$ (~95% confidence interval) or $2.4 \pm 0.3\,m$ (one standard deviation) for the total ocean-density effect. Note that changes in the salt budget would lead to greater uncertainties. Although not insignificant, this process alone is insufficient to balance the sea-
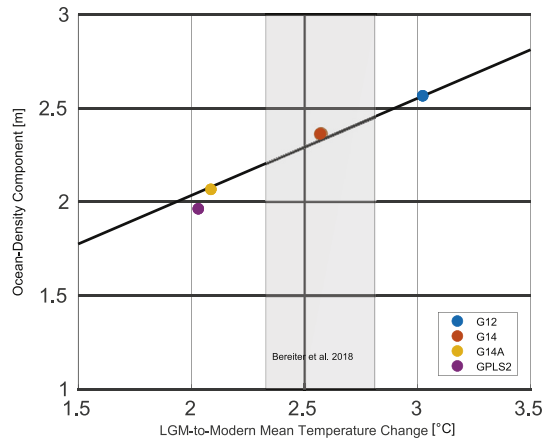
Fig. 4. Ocean-density effect $(\eta\text{-}\eta_{lice})$ as a function of temperature differential between the modern and LGM ocean $(\bar{\theta}_m\text{-}\bar{\theta}_g)$. G12, G14, G14A, and GPLS2 refer to the LGM ocean models of Gebbie (2012), Gebbie (2014), a modified version of Gebbie (2014), and Gebbie et al. (2015). Also shown in the gray box is the most recent estimate of global ocean temperature change since the LGM (Bereiter et al., 2018).

level budget at the LGM.

4. Groundwater changes

4.1. Background

Another factor often ignored in the total sea-level budget is the potential role of groundwater (Hay and Leslie, 1990). Currently, estimates for the contribution of groundwater depletion to 20th and 21st century sea-level rise vary between 0.075 and 0.8 mm/yr (Konikow, 2011; Wada et al., 2010), depending on the time frame used. However, few studies have addressed its potential to contribute to longer-term sea-level changes (Hay and Leslie, 1990). One recent assessment estimates the total groundwater stored in the continental crust to be 22.6 million km^3 (Gleeson et al., 2015). This volume of water is enough to raise sea levels by ~63 m assuming a global ocean area of 3.619×10^8 km^2 (Eakins and Sharman, 2010). A significant amount of that groundwater is known to be circulating within the hydrologic cycle with an estimated 210.5–837.6 million km^3 of water recharged since the LGM, although roughly a third of the current groundwater reservoirs are relicts from the LGM (Befus et al., 2017). Estimating the volume of groundwater at the LGM is a difficult task and direct measures of the groundwater table during the LGM are sparse. One approach to determining if groundwater could have played a significant role in balancing the sea-level budget at the LGM is to determine the maximum potential storage of the global groundwater basins.

4.2. Methods for estimating groundwater contributions to deglacial sea-level rise

We determined the maximum capacity of groundwater storage to contribute to lower sea levels at the LGM by estimating how much aquifer storage is empty at the present. We determined the potential storage of the largest 37 aquifers across the globe (WHYMAP, 2008; Margat, 2008) and included eight other major aquifers in regions with low modern water tables (e.g. the western US and interior Asia). In addition, we consider storage of groundwater in regions where permeability may not allow the subsurface materials to act as an aquifer; a lower value of porosity is used in these portions of the earth surface. We used the present-day water table elevations of Fan et al. (2013) (GW$_t$) and assumed a porosity

(n) of 0.2 for the sediments within the largest 37 basins and another 8 aquifers (Gleeson et al., 2015) and a porosity of 0.1 for areas outside the major aquifer basins in the following manner:

$$V_{gw} = \sum [\qquad\qquad\qquad (3)$$

where V$_{gw}$ represents the volume of groundwater storage, S$_{el}$ represents the surface elevation, and A represents the area of the groundwater aquifers or remaining land surface area. The land surface area was greater by approximately 6% during the LGM due to lower sea levels but that extra storage is now submerged and already saturated with either remnant freshwater from the LGM (Post et al., 2013) or seawater and not considered in our analysis. Although the porosity (0.2) is likely an overestimate, it provides an upper limit for the potential contribution of groundwater storage to lower sea levels during the LGM.

4.3. Groundwater changes results and discussion

Higher volumes of groundwater stored in the large aquifers shown in Fig. 5 during the LGM could account for approximately 0.6 m of sea-level rise equivalent with another 0.8 m of storage potential in the remaining land area (Fig. 5). This approach provides a maximum contribution. However, a number of factors could influence this estimate. First, these absolute storage volumes may underrepresent the total potential storage if the water table elevations of Fan et al. (2013) overestimate the true groundwater table, as suggested by Doll et al. (2016). Doll et al. (2016) point out the Fan et al. (2013) study was not dynamic nor did it take into account surface water interactions or capillary rise, both of which may lower groundwater levels resulting in an overestimation of the height of the true groundwater table and an underestimate of the total available storage.

Despite this potential underestimate, the 1.4 m estimate of global groundwater potential storage at the LGM most likely represents an upper bound and should be regarded as a maximum contribution for a number of other reasons. First, many areas appear to have experienced lower groundwater levels or recharge rates during the LGM not higher ones needed to sequester more groundwater at the LGM (Ferrera et al., 1999; Otto-Biesner et al., 2006; Befus et al., 2017). In addition, falling sea levels prior to the LGM exposed the shelf and likely drained now-submerged (and filled) aquifers during the LGM (Faure et al., 2002) resulting in lower groundwater storage. Similarly, lake levels across Asia and Africa reached their maximum size well after the LGM (Qin and Yu, 1998; Scholz et al., 2003), signifying a potential rising (not falling) of groundwater tables in these regions upon initial deglaciation. This said, groundwater tables likely varied by region as lakes, and thus local groundwater levels, in some regions were larger during the LGM (e.g. Lake Bonneville; Benson et al., 2011). Not only would this have influenced groundwater levels, it also would have provided additional terrestrial storage above the land surface in the form of lakes. Lake basins themselves are relatively small, with the largest modern lake, Lake Baikal, only storing enough water to raise sea levels by about 5 cm (Galaizy, 1993; cited in Osipov and Khlystove, 2010). Of note, Lake Baikal was lower during the LGM (Osipov and Khlystove, 2010). Proglacial lakes also pose a potential large source of water but most reached their maximum extent during the deglaciation and after the LGM, largely from the wasting of the LGM ice sheets. For example, Lake Agassiz-Ojibway reached its maximum extent 8–12 ka (Teller et al., 2002) and the Baltic Ice Lake reached its maximum extent 10.3–13.5 ka (Brunnberg, 1995). In a study based on GIA deformation in front of the Laurentide Ice Sheet, Lambeck et al. (2017) found space for large proglacial lakes
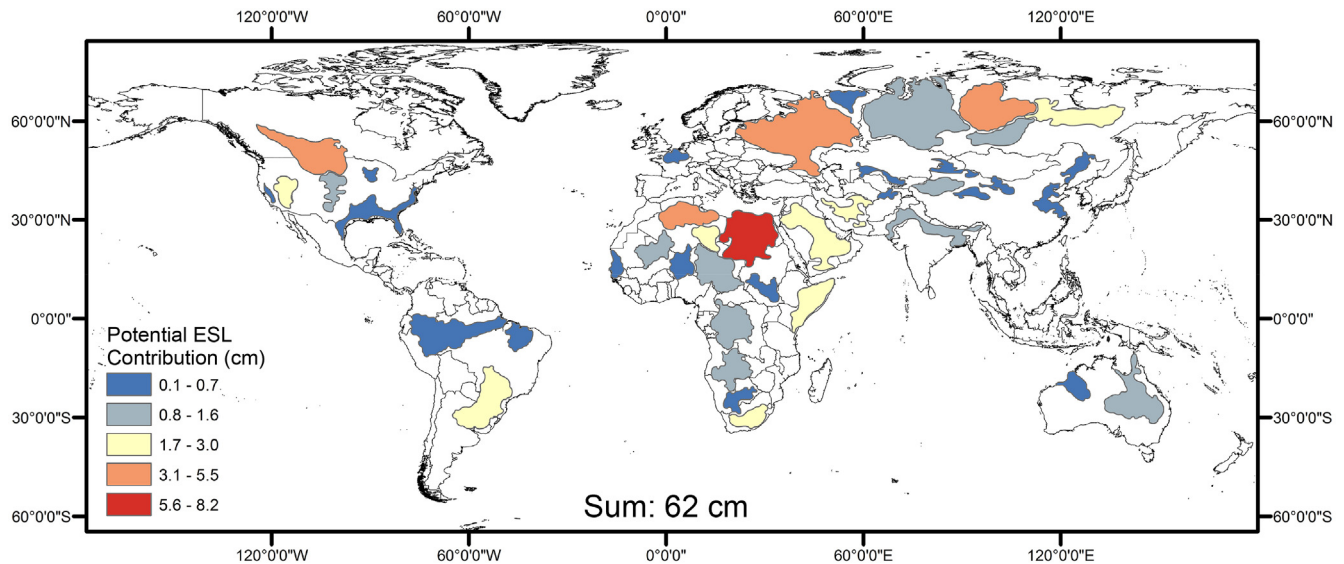
Fig. 5. Potential groundwater contributions to ice-equivalent sea level for the 37 largest aquifers as well as 8 other aquifers in arid to semiarid regions of the globe.

across north-central North America during the LGM but their volumes would contribute to a global sea-level rise equivalent of less than 1 m. A larger synthesis of lake-basin contributions to the LGM is warranted but from our work it appears that groundwater storage alone is far less than the 18.0 ± 9.6 m of sea-level equivalent needed to balance the LGM sea-level budget.

5. Updated missing ice estimate and directions forward

Taking ocean expansion and the possibility of a groundwater contribution into account reduces the "missing ice" to 15.6 ± 9.6 m (Figs. 2 and 3) with a nominal 95% confidence range of −2.6–34.9 m using the Monte Carlo simulation approach to the errors. Only 4.7% of simulations have enough ice to balance the sea-level budget (i.e., missing ice ≤ 0). These simulations include an LGM temperature change of 2.7±0.52 m (one standard deviation) and a groundwater change of 0 ± 0.7 m, which allows for uncertainty in the sign of change for groundwater at the LGM and a 2-δ range that includes the maximum possible groundwater storage increase. Increasing the uncertainty of the groundwater contribution to 0 ± 1.4 does not impact the mean estimate of missing ice but expands the 95% confidence interval to −2.8–35.1 m, with 4.9% of samples balancing the sea level budget. Our error analyses are relatively insensitive to uncertainty in the temperature and groundwater terms because these uncertainties are much smaller than the uncertainty associated with LGM ice volume. Even with a conservative approach that includes large uncertainties for ocean density and groundwater contributions, over 95% of Monte Carlo simulations require some contribution from missing ice.

As neither ocean expansion (Gebbie et al., in review) nor reduction in groundwater storage can account for more than a combined ~2.5–3.8 m of sea-level rise, the remaining 15.6 m of "missing ice" must be due to other processes or water reservoirs (Figs. 2 and 3). One possibility is that another ice sheet existed but has yet to be discovered. A potential location for such an ice sheet, mentioned by Clark and Tarasov (2014) and others earlier (Grosswald and Hughes, 2002), is eastern Siberia. However, despite attempts to find evidence for a significant LGM ice sheet in this region (Grosswald and Hughes, 2002), none has been found (Brigham-Grette et al., 2003; Gualtieri et al., 2003; Stauch and Lehmkuhl, 2010; Barr and Clark, 2011, 2012; Jakobsson et al.,

2014). A large ice sheet existed within the region at some point during the Pleistocene, but all evidence for this ice appears to predate the LGM (Niessen et al., 2013; O'Regan et al., 2017). Similarly, parts of the Arctic Ocean appear to have supported grounded ice, in the form of extensive ice shelves (Gasson et al., 2018). However, geomorphic evidence of past grounded ice and ice shelves again appear to predate the LGM and are thought to record extensive ice sheet and shelf growth during Marine Isotope Stage 6 (MIS6) (Jakobsson et al., 2016). Shallow portions of the Southern Ocean remain largely unexplored (e.g. Kerguelen Plateau, South Georgia), but they likely only held a few cms of sea-level equivalent at the LGM (Hall, 2009; Hodgson et al., 2014; Barlow et al., 2017; White et al., 2018), with one estimate of <14 cm sea-level equivalent (Denton and Hughes, 1981). However, more work is needed on these former Southern Ocean and Arctic ice centers.

A second possibility is that we have underestimated the contribution of one or more of the known ice sheets. Historically, Antarctica has been the "dumping ground" of missing ice. The continental shelves of the Ross and Weddell Seas have large areas that could hold as much as 11.3 and 13.1 m of sea-level equivalent, respectively (Bassett et al., 2007). However, paleogeographic models based on limited relative sea-level (RSL) data and mapping of grounded-ice features on the shelf and along nanutuks of the Antarctic Ice Sheet have failed to find evidence for an ice sheet large enough to balance the budget (Mackintosh et al., 2011; Whitehouse et al., 2012a; Golledge et al., 2013; Ivins et al., 2013; Briggs et al., 2014; Maris et al., 2014; Argus et al., 2014; The RAISED Consortium et al., 2014). Although, considering the limited amount of data and problems associated with dating materials in Antarctica, these models will likely be updated as more data become available. For example, the RSL data needed for GIA inversions are sparse across Antarctica with as few as 14 sites in a recent compilation (Whitehouse et al., 2012b) and nearly half of those confined to the Antarctic Peninsula leaving large expanses of the continent with little to no RSL constraints. This lack of data limits our ability to infer past ice-sheet change using a GIA modeling approach. In addition, parts of the Antarctic continent may be underlain by weaker rheology and/or be marked by Holocene ice-sheet fluctuations that most global GIA models do not consider (Ivins et al., 2000, 2011; Bradley et al., 2015; Wolstencroft et al., 2015; Simms et al., 2018; Kingslake et al., 2018). Furthermore,

all studies that seek to date former ice sheet extent within Antarctica are prone to uncertainties in radiocarbon reservoirs and inheritance associated with cosmogenic age dating.

The North American ice sheets also may have contained more ice at the LGM than current reconstructions, which contain an average of 76.0 m within our compilation. Lambeck et al. (2000) pointed out that although RSL data is readily available for the Holocene, the density of data is much lower during the early deglacial and as such leaves a large uncertainty in the volume of ice held at the LGM. Several models (Stokes et al., 2012; Gregoire et al., 2012; Lambeck et al., 2017; see review in Stokes, 2017) place up to 79 m of ice-equivalent sea-level rise within the ice sheets of North America and recent studies now suggest that the ice sheet reached the shelf edge along the Arctic Ocean (Stokes et al., 2017). However, this refinement alone most likely does not balance the ice-sheet budget. By only sampling North American ice sheet size estimates of 79–80 m (plus standard deviations of 5–8 m), the average estimate of missing ice is reduced to 12.3 m, and 93.5% of Monte Carlo samples require missing ice.

A third possibility is that ice volumes derived using a GIA modeling approach are biased low due to use of the wrong rheological model. It has long been known that global ice volumes inferred using a GIA model are strongly dependent on the assumed viscosity of the lower mantle (Milne et al., 1999, 2002; Lambeck et al., 2014). Caron et al. (2017) take this a step further and examine the effects of using a Burgers rheology within a GIA model — where the mantle is characterized by two different viscosities — rather than the more standard Maxwell rheology. They find significant differences in the ice mass required to fit observations of RSL when using a Burgers rheology compared with a Maxwell rheology, with the Burgers rheology solutions requiring more ice over North America and less ice over Antarctica compared with existing global ice sheet reconstructions. Unfortunately, it is not yet clear whether a Burgers, Maxwell, or power-law rheology provides the most realistic representation of the solid Earth; uncertainties associated with the choice of rheological model should be factored into future GIA model-derived estimates of LGM ice volume, or when applying a GIA correction to sea-level observations. Global ice sheet reconstructions (e.g. Peltier et al., 2015; Lambeck et al., 2014) are typically derived in conjunction with a preferred Earth rheology. If these rheologies are incorrect, or it is found that spatial variations in Earth rheology should be incorporated into global models (Austermann et al., 2013; A et al., 2013; Simms et al., 2018), then existing ice-sheet models will need to be refined.

Another possible solution to the missing ice problem is that our estimates of the amount of LGM sea-level lowering are too large. Despite the hundreds to thousands of RSL sites and indicators typically used to constrain ice sheet models (e.g. 512 sites for Tarasov et al., 2012; ~1000 indicators for Lambeck et al., 2014; 5720 indicators for Caron et al., 2017), estimates for the amount of sea-level lowering at the LGM are based on only three sites: Barbados, the Sunda Shelf, and the Bonaparte Gulf. Although all three datasets are based on careful work, each site has its complications. Barbados is a tectonically active island subject to vertical motion (Radtke and Schellmann, 2006), the indicative meaning of some of the sea-level indices from the Sunda Shelf remains uncertain (Hanebuth et al., 2009), and the cores within the Bonaparte Gulf may contain hiatuses (Shennan and Milne, 2003). More data constraining the LGM sea-level lowstand are needed from other locations far removed from the ice sheets. In addition, the uncertainty reported for the GIA-correction to far-field RSL sites is relatively low, reported in this study and by Spratt and Lisiecki (2016) as ±2 m, due to the absence of formal error bars in the estimates and the relatively few number of estimates. Future work should focus on determining how accurately these errors reflect the true

uncertainty in estimates of the magnitude of sea-level lowering including uncertainties in the GIA correction of far-field-based estimates.

6. Summary

A comparison between direct observations of LGM sea levels and the individual ice-sheet contributions to sea-level rise reveals a discrepancy of 18.1 ± 9.6 m of "missing ice". The ocean-density effect, including accounting for compression due to an additional ~130 m of water, and the potential storage of groundwater accounts for less than 3.9 m of the discrepancy. Thus, although significant, these factors cannot balance the LGM hydrological budget alone leaving 15.6 ± 9.6 m of ice-equivalent sea-level rise unaccounted for when accounting for appropriate uncertainties. One explanation for this discrepancy is that another source of meltwater must have existed at the LGM, either as a missing ice sheet, lakes, or as an underestimate of one or more of the already identified former ice sheets. Refinements to existing GIA models may provide insight into this third point. Future work should focus on improving the ice budgets of the known ice sheets, including further exploration of other potential ice-masses, as well as better constraining LGM sea-level change, groundwater levels and ocean temperature and salinity at the LGM.

References

A, G., Wahr, J., Zhong, S., 2013. Computations of the viscoelastic response of a 3-D compressible Earth to surface loading: an application to glacial isostatic adjustment in Antarctica and Canada. Geophys. J. Int. 192, 557–572.

Adkins, J.F., McIntyre, A., Schrag, D.P., 2002. The salinity, temperature, and d18O content of the glacial deep ocean. Science 298, 1769–1773.

Anderson, J.B., Shipp, S., Lowe, A.L., Wellner, J.S., Mosola, A.B., 2002. The antarctic ice sheet during the last glacial maximum and its subsequent retreat history: a review. Quat. Sci. Rev. 21, 49–70.

Anderson, J.B., Kirshner, A.E., Simms, A.R., 2013. Constraints on Antarctic Ice Sheet configuration during and following the last glacial maximum and its episodic contribution to sea-level rise. In: Hambrey, M.J., Barker, P.F., Barrett, P.J., Bowman, V., Davies, B., Smellie, J.L., Tranter, M. (Eds.), Antarctic Palaeoenvironments and Earth-surface Processes. The Geological Society, London.

Andrews, J.T., 1992. A case of missing water. Nature 358, 281.

Argus, D.F., Peltier, W.R., Drummond, R., Moore, A.W., 2014. The Antarctica component of postglacial rebound model ICE-6G_C (VM5a) based on GPS positioning, exposure age dating of ice thicknesses, and relative sea level histories. Geophys. J. Int. 198, 537–563.

Austermann, J., Mitrovica, J.X., Latychev, K., Milne, G., 2013. Barbados-based estimate of ice volume at Last Glacial Maximum affected by subducted plate. Nat. Geosci. 6, 553–557.

Barlow, N.L.M., Bentley, M.J., Spada, G., Evans, D.J.A., Hansom, J.D., Brader, M.D., White, J.S., Zander, A., Berg, S., 2016. Testing models of ice cap extent, South Georgia, sub-Antarctic. Quat. Sci. Rev. 154, 157–168.

Barr, I.D., Clark, C.D., 2011. Glaciers and climate in pacific far NE Russian during the last glacial maximum. J. Quat. Sci. 26, 227–237.

Barr, I.D., Clark, C.D., 2012. Late Quaternary glaciations in far NE Russia; combining moraines, topography, and chronology to assess regional and global glaciation synchrony. Quat. Sci. Rev. 53, 72–87.

Bassett, S.E., Milne, G.A., Bentley, M.J., Huybrechts, A., 2007. Modeling Antarctic sea-level data to explore the possibility of a dominant Antarctic contribution to meltwater pulse IA. Quat. Sci. Rev. 26, 2113–2127.

Befus, K.M., Jasechko, S., Luijendijk, E., Gleeson, T., Cardenas, M.B., 2017. The rapid yet uneven turnover of Earth's groundwater. Geophys. Res. Lett. 44, 073322.

Benson, L.V., Lund, S.P., Smoot, J.P., Rhode, D.E., Spencer, R.J., Verosub, K.L., Louderback, L.A., Johnson, C.A., Rye, R.O., Negrini, R.M., 2011. The rise and fall of Lake Bonneville between 45 and 10.5 ka. Quat. Int. 235, 57—69.

The RAISED Consortium, Bentley, M.J., O Cofaigh, C., Anderson, J.B., Conway, H., Davies, B., Graham, A.G.C., Hillenbrand, C.D., Hodgson, D.A., Jamieson, S.R., Larter, R.D., Mackintosh, A., Smith, J.A., Verleyen, E., Ackert, R.P., Bart, P.J., Berg, S., Brunstein, D., Canals, M., Colhoun, E.A., Crosta, X., Dickens, W.A., Domack, E.W., Dowdeswell, J.A., Dunbar, R., Ehrmann, W., Evans, J., Favier, V., Fink, D., Fogwill, C.J., Glasser, N.F., Gohl, K., Golledge, N.R., Goodwin, I., Gore, D.B., Greenwood, S.L., Hall, B.L., Hall, K., Hedding, D.W., Hein, A.S., Hocking, E.P., Jakobsson, M., Johnson, J.S., Jomelli, V., Jones, R.S., Klages, J.P., Kirstoffersen, Y., Kuhn, G., Leventer, A., Licht, K., Lilly, K., Lindow, J., Livingstone, S.J., Masse, G., McGlone, M.S., McKay, R.M., Melles, M., Miura, H., Mulvaney, R., Nel, W., Nitsche, F.O., O'Brien, P.E., Post, A.L., Roberts, S.J., Saunders, K.M., Selkirk, P.M., Simms, A.R., Spiegel, C., Stolldorf, T.D., Sugden, D.E., van der Putten, N., van Ommen, T., Verfaille, D., Vyverman, W., Wagner, B., White, D.A., Witus, A.E., Zwartz, D., 2014. A community-based geological reconstruction of antarctic ice sheet deglaciation since the last glacial maximum. Quat. Sci. Rev. 100, 1—9.

Bereiter, B., Shackleton, S., Baggenstos, D., Kawamura, K., Severinghaus, J.P., 2018. Mean global ocean temperatures during the last glacial transition. Nature 553, 39—44.

Bradley, S.L., Hindmarsh, R.C.A., Whitehouse, P.L., Bentley, M.J., King, M.A., 2015. Low post-glacial rebound rates in the Weddell Sea due to Late Holocene ice-sheet readvance. Earth Planet. Sci. Lett. 413, 79—89.

Briggs, R.D., Pollard, D., Tarasov, L., 2014. A data-constrained large ensemble analysis of Antarctic evolution since the Eemian. Quat. Sci. Rev. 103, 91—115.

Brigham-Grette, J., Gualtieri, L.M., Glushkova, O.Y., Hamilton, T.D., Mostoller, D., Kotov, A., 2003. Chlorine-36 and 14C chronology support a limited last glacial maximum across central Chukotka, northeastern Sibera, and no Beringian ice sheet. Quat. Res. 59, 386—398.

Brunnberg, L., 1995. The Baltic Ice Lake. Quat. Int. 28, 177—178.

Caron, L., Metivier, L., Greff-Lefftz, M., Fleitout, L., Rouby, H., 2017. Inverting glacial isostatic adjustment signal using Bayesian framework and two linearly relaxing rheologies. Geophys. J. Int. 209, 1126—1147.

Clark, P.U., Tarasov, L., 2014. Closing the sea level budget at the last glacial maximum. Proc. Natl. Acad. Sci. Unit. States Am. 111, 15861—15862.

Clark, P.U., Dyke, A.S., Shakun, J.D., Carlson, A.E., Clark, J., Wohlfarth, B., Mitrovica, J.X., Hostetler, S.W., McCabe, A.M., 2009. The last glacial maximum. Science 325, 710—714.

Colhoun, E.A., Mabin, M.C., Adamson, D.A., Kirk, R.M., 1992. Antarctic ice volume and contribution to sea-level fall at 20,000 yr BP from raised beaches. Nature 358, 316—319.

Denton, G.H., Hughes, T.J., 1981. The Last Great Ice Sheets. John Wiley & Sons.

Doll, P., Douville, H., Guntner, A., Schmied, H.M., Wada, Y., 2016. Modelling freshwater resources at the global scale: challenges and prospects. Surv. Geophys. 195—221, 2016.

Eakins, B.W., Sharman, G.F., 2010. Volumes of the World's Oceans from ETOPO1. NOAA National Geophysical Data Center, Boulder, CO.

Ehlers, J., Gibbard, P.L., Hughes, P.D., 2011. Quaternary Glaciations — Extent and Chronology. Elsevier, 1126 p.

Elderfield, H., Ferretti, P., Greaves, M., Cowhurst, S., McCave, I.N., Hodell, D., Piotrowski, A.M., 2012. Evolution of ocean temperature and ice volume through the mid-Pleistocene climate transition. Science 337, 704—709.

Fairbanks, R.G., 1989. A 17,000 year glacio-eustatic sea-level record: influence of glacial melting on the Younger Dryas Event and deep-ocean circulation. Nature 342, 637—642.

Fan, Y., Li, H., Miguez-Macho, G., 2013. Global patterns of groundwater table depth. Science 339.

Faure, H., Walter, R.C., Grant, D.R., 2002. The coastal oasis: ice age springs on emerged continental shelves. Global Planet. Change 33, 47—56.

Ferrera, I., Harrison, S.P., Prentice, I.C., Ramstein, G., Guiot, J., Bartlein, P.J., Bonnefille, R., Bush, M., Cramer, W., von Grafenstein, U., Holmgren, K., Hooghiemstra, H., Hope, G., Jolly, D., Lauritzen, S.-E., Ono, Y., Pinot, S., Stute, M., Yu, G., 1999. Tropical climates at the Last Glacial Maximum: a new synthesis of terrestrial palaeoclimate data. I. Vegetation, lake-levels and geochemistry. Clim. Dynam. 15, 823—856.

Fleming, K., Lambeck, K., 2004. Constraints on the Greenland ice sheet since the last glacial maximum from sea-level observations and glacial rebound models. Quat. Sci. Rev. 23, 1053—1077.

Galaziy, G.I., 1993. Atlas of Lake Baikal. Roskartografia Press.

Gasson, E.G.W., DeCanto, R.M., Pollard, D., Clark, C.D., 2018. Numerical simulations of a kilometre-thick Arctic ice shelf consistent with ice grounding observations. Nat. Commun. 9, 1—9.

Gebbie, G., 2012. Tracer transport timescales and the observed Atlantic-Pacific lag in the timing of the last Termination. Paleoceanography 27, PA3225.

Gebbie, G., 2014. How much did glacial North Atlantic water shoal? Paleoceanography 29, 190—209.

Gebbie, G., Peterson, C.D., Lisiecki, L.E., Spero, H.J., 2015. Global-mean marine del13C and its uncertainty in a glacial state estimate. Quat. Sci. Rev. 125, 144—159.

Gleeson, T., Befus, K.M., Jasechko, S., Luijendijk, E., Cardenas, M.B., 2015. The global volume and distribution of modern groundwater. Nat. Geosci. 9.

Golledge, N.R., Levy, R.H., McKay, R.M., Fogwill, C.J., White, D.A., Graham, A.G.C., Smith, J.A., Hillenbrand, C.D., Licht, K.J., Denton, G.H., Ackert, R.P.J., Maas, S.M., Hall, B.L., 2013. Glaciology and geological signature of the last glacial maximum

antarctic ice sheet. Quat. Sci. Rev. 78, 225—247.

Golledge, N.R., Menviel, L., Carter, L., Fogwill, C.J., England, M.H., Cortese, G., Levy, R.H., 2014. Antarctic contribution to meltwater pulse 1A from reduced Southern Ocean overturning. Nat. Commun. 5 (5107), 1—10.

Gomez, N., Pollard, D., Mitrovica, J.X., 2013. A 3-D coupled ice sheet - sea level model applied to Antarctica through the last 40 ky. Earth Planet. Sci. Lett. 384, 88—99.

Gregoire, L.J., Payne, A.J., Valdes, P.J., 2012. Deglacial rapid sea level rises caused by ice-sheet saddle collapses. Nature 487, 219—222.

Grosswald, M.G., Hughes, T.J., 2002. The Russian component of an arctic ice sheet during the last glacial maximum. Quat. Sci. Rev. 21, 121—146.

Gualtieri, L., Vartanyan, S., Brigham-Grette, J., Anderson, P.M., 2003. Pleistocene raised marine deposits on Wrangel Island, northeast Siberia and implications for the presence of an East Siberian ice sheet. Quat. Res. 59, 399—410.

Hall, B., 2009. Holocene glacial history of Antarctica and the sub-Antarctic islands. Quat. Sci. Rev. 28, 2213—2230.

Hanebuth, T., Stattegger, K., Grootes, P.M., 2000. Rapid flooding of the Sunda Shelf: a late-glacial sea-level record. Science 288, 1033—1035.

Hanebuth, T.J.J., Stattegger, K., Bojanowski, A., 2009. Termination of the last glacial maximum sea-level lowstand: the Sunda-shelf data revisited. Global Planet. Change 66, 76—84.

Hay, W.W., Leslie, M.A., 1990. Could Possible Changes in Global Groundwater Reservoir Cause Eustatic Sea-level Fluctuations?, Sea-level Change. The National Academies, Washington D.C., pp. 161—170

Hodgson, D.A., Graham, A.G., Griggiths, H.J., Roberts, S.J., O Cofaigh, C., Bentley, M.J., Evans, D.J., 2014. Glacial history of sub-Antarctic South Georgia based on the submarine geomorphology of its fjords. Quat. Sci. Rev. 89, 129—147.

Hughes, A.L.C., Gyllencreutz, R., Lohne, O.S., Mangerud, J., Svendsen, J.I., 2016. The last Eurasian ice sheets - a chronological database and time-slice reconstruction, DATED-1. Boreas 45, 1—45.

Huybrechts, P., 2002. Sea-level changes at the LGM from ice-dynamic reconstructions of the Greenland and Antarctic ice sheets during the glacial cycles. Quat. Sci. Rev. 21, 203—231.

Ivins, E.R., James, D.P., 2005. Antarctic glacial isostatic adjustment: a new assessment. Antarct. Sci. 17, 541—553.

Ivins, E.R., Raymond, C.A., James, T.S., 2000. The influence of 5,000 year-old and younger glacial mass variability on present-day crustal rebound in the Antarctic Peninsula. Earth Planets Space 52, 1023—1029.

Ivins, E.R., James, T.S., Wahr, J., Schrama, E.J.O., Landerer, F.W., Simon, K.M., 2013. Antarctic contribution to sea level rise observed by GRACE with improved GIA correction. J. Geophys. Res. 118, 1—16.

Jakobsson, M., Andreassen, K., Bjarnadottir, L.R., Dove, D., Dowdeswell, J.A., England, J.H., Funder, S., Hogan, K., Ingolfsson, O., Jennings, A., Larsen, N.K., Kirchner, N., Landvik, J.Y., Mayer, L., Mikkelsen, N., Moller, P., Niessen, F., Nilsson, J., O'Regan, M., Polyak, L., Norgaard-Pedersen, N., Stein, R., 2014. Arctic Ocean glacial history. Quat. Sci. Rev. 92, 40—67.

Jakobsson, M., Nilsson, J., Anderson, L., Backman, J., Bjork, G., Cronin, T.M., Kirchner, N., Koshurnikov, A., Mayer, L., Noormets, R., O'Regan, M., Stranne, C., Ananiev, R., Macho, N.B., Cherniykh, D., Coxall, H., Eriksson, B., Floden, T., Gemery, L., Gustafsson, O., Jerram, K., Johansson, C., Khortov, A., Mohammad, R., Semiletov, I., 2016. Evidence for an ice shelf covering the central Arctic Ocean during the penultimate glaciation. Nat. Commun. 7, 10365.

Kageyama, M., Laine, A., Abe-Ouchi, A., Braconnot, P., Cortijo, E., Crucifix, M., De Vernal, A., Guiot, J., Hewitt, C.D., Kitoh, A., Kucera, M., Marti, O., Ohgaito, R., Otto-Bliesner, B., Peltier, W.R., Rosell-Mele, A., Vettoretti, G., Weber, S.L., Yu, Y., Members, M.P., 2006. Last Glacial Maximum temperature over the North Atlantic, Europe and western Siberia: a comparison between PMIP models, MARGO sea-surface temperatures and pollen-based reconstructions. Quat. Sci. Rev. 25.

Khan, S.A., Sasgen, I., Bevis, M., van Dam, T., Bamber, J.L., Wahr, J., Willis, M., Kjaer, K.H., Wouters, B., Helm, V., Csatho, B., Fleming, K., Bjork, A.A., Aschwanden, A., Knudsen, P., Munneke, P.K., 2016. Geodetic measurements reveal similarities between post-Last Glacial Maximum and present-day mass loss from the Greenland ice sheet. Sci. Adv. 2, e1600931.

Kingslake, J., Scherer, R.P., Albrecht, T., Coenen, J., Powell, R.D., Reese, R., Stansell, N.D., Tulaczyk, S., Wearing, M.G., Whitehouse, P.L., 2018. Extensive retreat and re-advance of the west antarctic ice sheet during the Holocene. Nature 558, 430—434.

Konikow, L.F., 2011. Contribution of global groundwater depletion since 1900. Geophys. Res. Lett. 38, L17401.

Lambeck, K., Chappell, J., 2001. Sea level change through the last glacial cycle. Science 292, 679—686.

Lambeck, K., Purcell, A., 2005. Sea-level change in the Mediterranean Sea since the LGM: model predictions for tectonically stable areas. Quat. Sci. Rev. 24, 1969—1988.

Lambeck, K., Yokoyama, Y., Johnston, P., Purcell, A., 2000. Global ice volumes at the last glacial maximum and early Lateglacial. Earth Planet. Sci. Lett. 181, 513—527.

Lambeck, K., Purcell, A., Funder, S., Kjaer, K., Larsen, E., Moller, P., 2006. Constraints on the Late Saalian to early Middle Weichselian ice sheet of Eurasia from field data and rebound modelling. Boreas 35, 539—575.

Lambeck, K., Purcell, A., Flemming, N.C., Vita-Finzi, C., Alsharekh, A.M., Bailey, G.N., 2011. Sea level and shoreline reconstructions for the Red Sea: isostatic and tectonic considerations and implications for hominin migration out of Africa. Quat. Sci. Rev. 30, 3542—3574.

Lambeck, K., Rouby, H., Purcell, A., Sun, Y., Sambridge, M., 2014. sea level and global

ice volumes from the last glacial maximum to the Holocene. Proc. Natl. Acad. Sci. Unit. States Am. 111 (15), 296-215,303.

Lambeck, K., Purcell, A., Zhao, S., 2017. The North American Late Wisconsin ice sheet and mantle viscosity from glacial rebound analyses. Quat. Sci. Rev. 158, 172–210.

Lecavalier, B.S., Milne, G.A., Simpson, M.J.R., Wake, L., Huybrechts, P., Tarasov, L., Kjeldsen, K.K., Funder, S.V., Long, A.J., Woodroffe, S.A., Dyke, A.S., Larsen, N.K., 2014. A model of Greenland ice sheet deglaciation constrained by observations of relative sea level and ice extent. Quat. Sci. Rev. 102, 54–84.

Lisiecki, L.E., Raymo, M.E., 2005. A Pliocene-Pleistocene stack of 57 globally distributed benthic $\delta^{18}O$ records. Paleoceanography 20. PA1003.

Mackintosh, A., Golledge, N., Domack, E.W., Dunbar, R., Leventer, A., White, D., Pollard, D., DeConto, R., Fink, D., Zwartz, D., Gore, D., Lavoie, C., 2011. Retreat of the East Antarctic ice sheet during the last glacial maximum. Nat. Geosci. 4, 195–202.

Margat, J., 2008. Great aquifer systems of the world. In: Chery, L., de Marsily, G. (Eds.), Aquifer Systems Management: Darcy's Legacy in a World of Impending Water Shortage. Taylor & Francis, New York, pp. 105–116.

Maris, M.N.A., De Boer, B., Ligtenberg, S.R.M., Crucifix, M., Van de Berg, W.J., Oerlemans, J., 2014. Modeling the evolution of the Antarctic ice sheet since the last interglacial. Cryosphere 8, 1347–1360.

Members, M.P., 2009. Constraints on the magnitude and patterns of ocean cooling at the Last Glacial Maximum. Nat. Geosci. 2, 127–132.

Milne, G.A., Mitrovica, J.X., Davis, J.L., 1999. Near-field hydro-isostasy; implications of a revised sea-level equation. Geophys. J. Int. 139, 464–482.

Milne, G.A., Mitrovica, J.X., Schrag, D.P., 2002. Estimating past continental ice volume from sea-level data. Quat. Sci. Rev. 21, 361–376.

Mitrovica, J.X., 2003. Recent controversies in predicting post-glacial sea-level change. Quat. Sci. Rev. 22, 127–133.

Mix, A.C., 1987. Chapter 6: the oxygen-isotope record of glaciation. In: Ruddiman, W.F., Wright, H.E.J. (Eds.), North America and Adjacent Oceans during the Last Deglaciation. Geological Society of America, Boulder, CO, pp. 111–135.

Munk, W., 2003. Ocean freshening, sea level rising. Science 300, 2041–2043.

Nakada, M., Lambeck, K., 1988. The melting history of the late Pleistocene Antarctic ice sheet. Nature 333, 36–40.

Nakada, M., Kimura, R., Okuno, J., Moriwaki, K., Miura, H., Maemoku, H., 2000. Late Pleistocene and Holocene melting history of the Antarctic ice sheet derived from sea-level variations. Mar. Geol. 167, 85–103.

Nakada, M., Okuno, J., Yokoyama, Y., 2016. Total meltwater volumes since the Last Glacial Maximum and viscosity structure of Earth's mantle inferred from relative sea level changes at Barbados and Bonaparte Gulf and GIA-induced J2. Geophys. J. Int. 204, 1237–1253.

Niessen, F., Hong, J.K., Hegewald, A., Matthiessen, J., Stein, R., Kim, H., Kim, S., Jensen, L., Jokat, W., Nam, S.-I., Kang, S.-H., 2013. Repeated Pleistocene glaciation of the East Siberian continental margin. Nat. Geosci. 6, 842–846.

O'Regan, M., Backman, J., Barrientos, N., Cronin, T.M., Gemery, L., Kirchner, N., Mayer, L.A., Nilsson, J., Noormets, R., Pearce, C., Semiletov, I., Stranne, C., Jakobsson, M., 2017. The De Long Trough: a newly discovered glacial trough on the East Siberian continental margin. Clim. Past 13, 1269–1284.

Osipov, E.Y., Khlystov, O.M., 2010. Glaciers and meltwater flux to Lake Baikal during the last glacial maximum. Palaeogeogr. Palaeoclimatol. Palaeoecol. 294, 4–15.

Otto-Biesner, B.L., Brady, E.C., Clauzet, G., Tomas, R., Levis, S., Kothavala, Z., 2006. Last glacial maximum and Holocene climate in CCSM3. J. Clim. 19, 2526–2544.

Patton, H., Hubbard, A., Andreassen, K., Winsborrow, M., Stroeven, A.P., 2016. The build-up, configuration, and dynamical sensitivity of the Eurasian ice-sheet complex to Late Weichselian climatic and oceanic forcing. Quat. Sci. Rev. 153, 97–121.

Peltier, W.R., 1994. Ice age paleotopography. Science 265, 195–201.

Peltier, W.R., 2004. Global glacial isostasy and the surface of the Ice-Age Earth: the ICE-5G (VM2) model and GRACE. Annu. Rev. Earth Planet Sci. 32, 111–149.

Peltier, W.R., Fairbanks, R.G., 2006. Global glacial ice volume and Last Glacial Maximum duration from an extended Barbados sea level record. Quat. Sci. Rev. 25, 3322–3337.

Peltier, W.R., Argus, D.F., Drummond, R., 2015. Space geodesy constrains ice age terminal deglaciation: the global ICE-6G_C (VM5a) model. J. Geophys. Res.: Solid Earth 120, 450–487.

Post, V.E.A., Groen, J., Kooi, H., Person, M., Ge, S., Edmunds, W.M., 2013. Offshore fresh groundwater reserves as a global phenomenon. Nature 504, 71–78.

Qin, B., Yu, G., 1998. Implications of lake level variations at 6 ka and 18 ka in mainland Asia. Global Planet. Change 18, 59–72.

Radtke, U., Schellmann, G., 2006. Uplift history along the Clermont Nost Traverse on the West Coast of Barbados during the last 500,000 years - implications for paleo-sea level reconstructions. J. Coast Res. 22, 350–360.

Root, B.C., Tarasov, L., Van der Wal, W., 2015. GRACE gravity observations constrain Weichselian ice thickness in the Barents Sea. Geophys. Res. Lett. 42, 3313–3320.

Scholz, C.A., King, J.W., Ellis, G.S., Swart, P.K., Stager, J.C., Colman, S.M., 2003. Paleolimnology of lake Tanganika, East Africa, over the past 100 k yr. J. Paleolimnol.

30, 139-2003.

Shennan, I., Milne, G., 2003. sea-level observations around the last glacial maximum from the Bonaparte Gulf, NW Australia. Quat. Sci. Rev. 22, 1543–1547.

Shepherd, A., Ivins, E.R., A, G., Barletta, V., Bentley, M.J., Bettadpur, S., Briggs, K.H., Bromwich, D.H., Forsberg, C.F., Galin, N., Horwath, M., Jacobs, S., Joughin, I., King, M.A., Lenaerts, J.T.M., Li, J., Ligtenberg, S.R.M., Luckman, A., Luthcke, S.B., McMillan, M., Meister, R., Milne, G., Mouginot, J., Muir, A., Nicolas, J.P., Paden, J., Payne, A.J., Pritchard, H., Rignot, E., Rott, H., Sorenson, L.S., Scambos, T.A., Scheuchl, B., Schrama, E.J.O., Smith, B., Sundal, A.V., Van Angelen, J.H., Van de Berg, W.J., Van den Broeke, M.R., Vaughan, D.G., Velicogna, I., Wahr, J., Whitehouse, P.L., Wingham, D.J., Yi, D., Young, D., Zwally, H.J., 2012a. A reconciled estimate of ice-mass balance. Science 338, 1182–1189.

Shepherd, A., Ivins, E.R., A, G., Barletta, V.R., Bentley, M.J., Bettadpur, S., Briggs, K.H., Bromwich, D.H., Forsberg, R., Galin, N., Horwath, M., Jacobs, S., Joughin, I., King, M.A., Lenaerts, J.T.M., Li, J., Ligtenberg, S.R.M., Luckman, A., Luthcke, S.B., McMillan, M., Meister, R., Milne, G., Mouginot, J., Muir, A., Nicolas, J.P., Paden, J., Scambos, T.A., Scheuchl, B., Schrama, E.J.O., Smith, B., Sundal, A.V., van Angelen, J.H., van de Berg, W.J., Van den Broeke, M.R., Vaughan, D.G., Velicogna, I., Wahr, J., Whitehouse, P.L., Wingham, D.J., Yi, D., Young, D., Zwally, H.J., 2012b. A reconciled estimate of ice-mass balance. Science 338, 1182–1189.

Simms, A.R., Whitehouse, P.L., Simkins, L.M., Nield, G., DeWitt, R., Bentley, M.J., 2018. Late Holocene relative sea levels near Palmer Station, northern Antarctic Peninsula, strongly controlled by late Holocene ice-mass changes. Quat. Sci. Rev. 199, 49–59.

Simon, K.M., James, T.S., Henton, J.A., Dyke, A.S., 2016. A glacial isostatic adjustment model for the central and northern Laurentide Ice Sheet based on relative sea level and GPS measurements. Geophys. J. Int. 205, 1618–1636.

Simpson, M.J.R., Milne, G.A., Huybrechts, P., Long, A.J., 2009. Calibrating a glaciological model of the Greenland ice sheet from the Last Glacial Maximum to present-day using field observations of relative sea level and ice extent. Quat. Sci. Rev. 28, 1631–1657.

Spratt, R.M., Lisiecki, L.E., 2016. A Late Pleistocene sea level stack. Clim. Past 12, 1079–1092.

Stauch, G., Lehmkuhl, F., 2010. Quaternary glaciations in the Verkhoyansk mountains, northeast Siberia. Quat. Res. 74, 145–155.

Stokes, C.R., 2017. Deglaciation of the Laurentide ice sheet from the last glacial maximum. Cuadernos de Investigacion Geografica (Geographical Research Letters) 43, 377–428.

Stokes, C.R., Tarasov, L., Dyke, A., 2012. Dynamics of the North American ice sheet complex during its inception and build-up to the last glacial maximum. Quat. Sci. Rev. 50, 86–104.

Stokes, C.R., Marigold, M., Clark, C.D., Tarasov, L., 2017. Ice stream activity scaled to ice sheet volume during Laurentide Ice Sheet deglaciation. Nature 530, 322–326.

Tarasov, L., Peltier, W.R., 2002. Greenland glacial history and local geodynamic consequences. Geophys. J. Int. 150, 198–229.

Tarasov, L., Dyke, A.S., Neal, R.M., Peltier, W.R., 2012. A data-calibrated distribution of deglaical chronologies for the North American ice complex from glaciological modeling. Earth Planet. Sci. Lett. 315–316, 30–40.

Teller, J.T., Leverington, D.W., Mann, J.D., 2002. Freshwater outbursts to the oceans from glacial Lake Agassiz and their role in climate change during the last deglaciation. Quat. Sci. Rev. 21, 879–887.

Wada, Y., van Beek, L.P.H., van Kempen, C.M., Reckman, J.W.T.M., Vasak, S., Bierkens, M.F.P., 2010. Global depletion of groundwater resources. Geophys. Res. Lett. 37, L20402.

White, D.A., Bennike, O., Melles, M., Berg, S., Binnie, S.A., 2018. Was South Georgia covered by an ice cap during the last glacial maximum? In: Siegert, M.J., Jamieson, S.S.R., White, D.A. (Eds.), Exploration of Subsurface Antarctica: Uncovering Past Changes and Modern Processes. Geological Society, London, London, pp. 49–59.

Whitehouse, P.L., Bentley, M.J., Le Brocq, A.M., 2012a. A deglacial model for Antarctica: geological constraints and glaciological modelling as a basis for a new model of Antarctic glacial isostatic adjustment. Quat. Sci. Rev. 32, 1–24.

Whitehouse, P.L., Bentley, M.J., Milne, G.A., King, M.A., Thomas, I.D., 2012b. A new glacial isostatic adjustment model for Antarctica: calibrated and tested using observations of relative sea-level change and present-day uplift rates. Geophys. J. Int. 190, 1464–1482.

WHYMAP, 2008. Groundwater Resources of the World. BGR/UNESCO, Paris.

Wolstencroft, M., King, M.A., Whitehouse, P.L., Bentley, M.J., Nield, G.A., King, E.C., McMillan, M., Shepherd, A., Barletta, V., Bordoni, A., Riva, R.E.M., Didova, O., Gunter, B.C., 2015. Uplift rates from a new high-density GPS network in Palmer Land indicate significant late Holocene ice loss in the southwestern Weddell Sea. Geophys. J. Int. 203, 737–754.

Yokoyama, Y., Lambeck, K., De Dekker, P., Johnston, P., Fifield, L.K., 2000. Timing of the last glacial maximum from observed sea-level minima. Nature 406, 713–716.